RESEARCH PAPER

Nucleus 4:5, 399–409; September/October 2013; © 2013 Landes Bioscience

Developmental regulation of linkers of the nucleoskeleton to the cytoskeleton during mouse postnatal retinogenesis

David S Razafsky[1], Candace L Ward[1], Thorsten Kolb[2], and Didier Hodzic[1,*]

[1]Department of Ophthalmology and Visual Sciences; Washington University School of Medicine; St Louis, MO USA; [2]Division of Molecular Genetics; German Cancer Research Center (DKFZ); Heidelberg, Germany

Keywords: lamins, Sun proteins, nesprins, KASH domain, retinogenesis, nuclear envelope

Abbreviations: CPs, cone photoreceptors; RPs, rod photoreceptors; HCs, horizontal cells; BPs, bipolar cells; ACs, amacrine cells; RGC, retinal ganglion cells; RPCs, retinal progenitor cells; ONL, outer nuclear layer; INL, inner nuclear layer; OPL, outer plexiform layer; IPL, inner plexiform layer; GCL, ganglion cell layer; NBL, neuroblast layer; LINC, linkers of the nucleoskeleton to the cytoskeleton; NE, nuclear envelope; PNS, perinuclear space; KASH, Klarsicht/Anc-1, Syne Homology; SUN, Sad1/Unc84; Nesprins, nuclear envelope spectrins; CNS, central nervous system; IKNM, interkinetic nuclear migration; ISH, in situ hybridization; IF, immunofluorescence; PCR, polymerase chain reaction

Sun proteins and nesprins are two families of proteins whose direct interactions across the nuclear envelope provide for the core of linkers of the nucleoskeleton to the cytoskeleton (LINC complexes) that physically connect the nucleus interior to cytoskeletal networks. Whereas LINC complexes play essential roles in nuclear migration anchorage and underlie normal CNS development, the developmental regulation of their composition remains largely unknown. In this study, we examined the spatiotemporal expression of lamins, Sun proteins and nesprins during postnatal mouse retinal development. Whereas retinal precursor cells mostly express B-type lamins, Sun1 and high molecular weight isoforms of Nesprins, post-mitotic retinal cells are characterized by a drastic downregulation of the latter, the expression of A-type lamins and the strong induction of a specific isoform of Nesprin1 late in retinal development. Importantly, our results emphasize different spatiotemporal expression for Nesprin1 and Nesprin2 and further suggest an important role for KASH-less isoforms of Nesprin1 in the CNS. In conclusion, the transition from retinal precursor cells undergoing interkinetic nuclear migration to post-mitotic retinal cells undergoing nuclear translocation and/or anchorage is accompanied by a profound remodeling of LINC complexes composition. This remodeling may reflect different requirements of nuclear dynamics at different stages of CNS development.

Introduction

Many CNS tissues are organized into various numbers of nuclear layers separated by regions of synaptic connections. CNS lamination is well illustrated by the organization of the mammalian retina that is composed of three layers of nuclei: the outer and inner nuclear layers (ONL and INL, respectively) and the ganglion cell layer (GCL). The ONL contains nuclei of photosensitive rods and cones while the INL consists of horizontal, bipolar, amacrine and Müller cells, the latter providing for the retinal glia. The GCL is composed of retinal ganglion cells (RGCs) whose axons' bundling form the optic nerve that relays visual cues to higher brain processing centers. The outer and inner plexiform layers (OPL and IPL, respectively) correspond to synaptic contact zones between photoreceptors and second order neurons and between second order neurons and the GCL, respectively. During differentiation, a complex combination of intrinsic and extrinsic cues ultimately results in the determination of retinal cells fates (reviewed in ref. 1). The first peak of differentiation in the retina is initiated at ~E11.5 and includes the overlapping birth of RGC, amacrine, horizontal and cone precursor cells. The second wave of differentiation is initiated within the first postnatal week and gives rise to rods, bipolar cells, and Müller glia.[2]

Proper CNS lamination requires specific types of nuclear movements during the proliferative and post-mitotic phases of retinal development. The first type of nuclear movement is interkinetic nuclear migration (IKNM) that consists of cell cycle-dependent oscillations of nuclei within the cytoplasm of retinal progenitor cells (RPCs).[1,3-5] Because nuclei migrate basally during G1 and apically during G2, mitoses take place on the apical side whereas S-phase is initiated on the basal side of neuroepithelia. The second type of nuclear movement associated with CNS development is nuclear translocation. In the developing brain, the latter consist of saltatory nuclear movements within post-mitotic

*Correspondence to: Didier Hodzic; Email: Hodzicd@vision.wustl.edu
Submitted: 07/24/13; Revised: 08/19/13; Accepted: 08/22/13
http://dx.doi.org/10.4161/nucl.26244

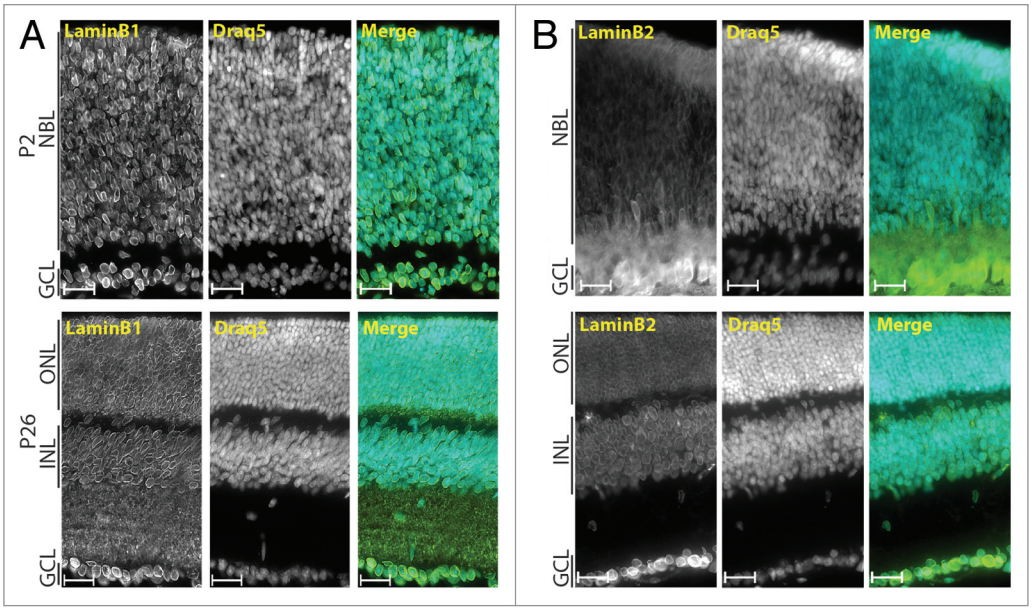

Figure 1. B-type lamins are ubiquitously and homogenously expressed in the developing retina. Immunolocalization of LaminB1 (**A**) and LaminB2 (**B**) in P2 (top) and P26 (bottom) retinas counterstained with DRAQ5. Scale bars: 25μm.

migrating precursors.[6] Failure of nuclear translocation within neuronal precursor cells underlies lissencephalies, a variety of severe brain developmental defects characterized by abnormal cortical lamination.[7] Whereas the role of nuclear translocation is still poorly understood in retinal lamination, severe ocular defects that accompany different types of lissencephalies strongly suggest that nuclear translocation is also essential to retinal lamination.[8] This is further supported by dramatic bidirectional post-mitotic migration during retinogenesis.[9-12] For example, from P4 to P11, cone nuclei are scattered at variable positions within the apical two-thirds of the developing ONL before migrating toward the apical edge of the ONL.[9] Likewise, at ~E14.5 horizontal cell (HC) precursors migrate basally toward the developing GCL, overshooting their presumptive position within the neuroblast layer (NBL) before migrating apically to reach their final laminar position on the apical side of the INL.[10-12]

It is now well established that cytoskeletal and nuclear envelope (NE) proteins play a central role in nuclear migration and anchorage.[13-16] The NE is composed of an inner and outer nuclear membrane (INM and ONM, respectively) that connect at nuclear pores and delineate the perinuclear space (PNS). The ONM is an extension of the rough ER and the INM adheres to the nuclear lamina that is composed of A- and B-type lamins.[17-19] Linkers of the nucleoskeleton to the cytoskeleton (LINC complexes) are large macromolecular scaffolds that span the NE and connect the nuclear lamina to components of the cytoplasmic cytoskeleton.[19-21] The backbone of LINC complexes consists of interactions between two families of transmembrane proteins: Sun proteins (Sad1/Unc84) and nesprins (nuclear envelope spectrins, also known as Syne proteins for synaptic nuclear envelope protein). In mammals, Sun1 and Sun2, which are encoded by two distinct genes, are integral transmembrane proteins of the INM whose N-terminal nucleoplasmic region interacts directly with nuclear lamins.[22-24] Within the PNS, the highly conserved C-terminal SUN domain interacts directly with the evolutionary-conserved KASH (Klarsicht/Anc-1, Syne homology) domain located at the C-terminus of nesprins. Nesprin proteins are integral transmembrane proteins of the ONM whose cytoplasmic regions range from ~50 kDa to ~1 MDa and interact with a variety of cytoskeletal elements and molecular motors.[25-29]

Evidence from several species suggests that an evolutionary-conserved "molecular axis" consisting of lamins/Sun proteins/nesprins/cytoplasmic cytoskeletal elements regulates nuclear movement and anchorage.[13,21] For example, in *D. melanogaster,* the migration of photoreceptor precursor nuclei is similarly altered by the mutation of $LaminDm_0$ (B-type lamin), klaroid (SUN), Klarsicht (KASH) or the glued subunit of dynactin.[30-33] Likewise in zebrafish, either the overexpression of p50/dynamitin, which dissociates the dynactin complex, or the overexpression of the KASH domain, which interferes with endogenous LINC complex assembly in a dominant-negative manner, lead to mispositioning of photoreceptor nuclei.[34] Finally, we and others have shown in complementary mouse models that SUN-KASH interactions play an important role in the migratory behavior of cone photoreceptor nuclei.[13,14] Despite this wealth of information, the developmental regulation of LINC complexes components remains poorly characterized. In the current study, we have characterized the spatiotemporal expression pattern of A- and B-type lamins, Sun1 and 2, as well as nesprin1 and 2 during postnatal retinal development. Our results indicate that the composition of LINC complexes varies tremendously in a developmental and cell type-specific manner.

Results

Expression pattern of lamins in the developing retina. To investigate the regulation of A- and B-type lamins during retinal

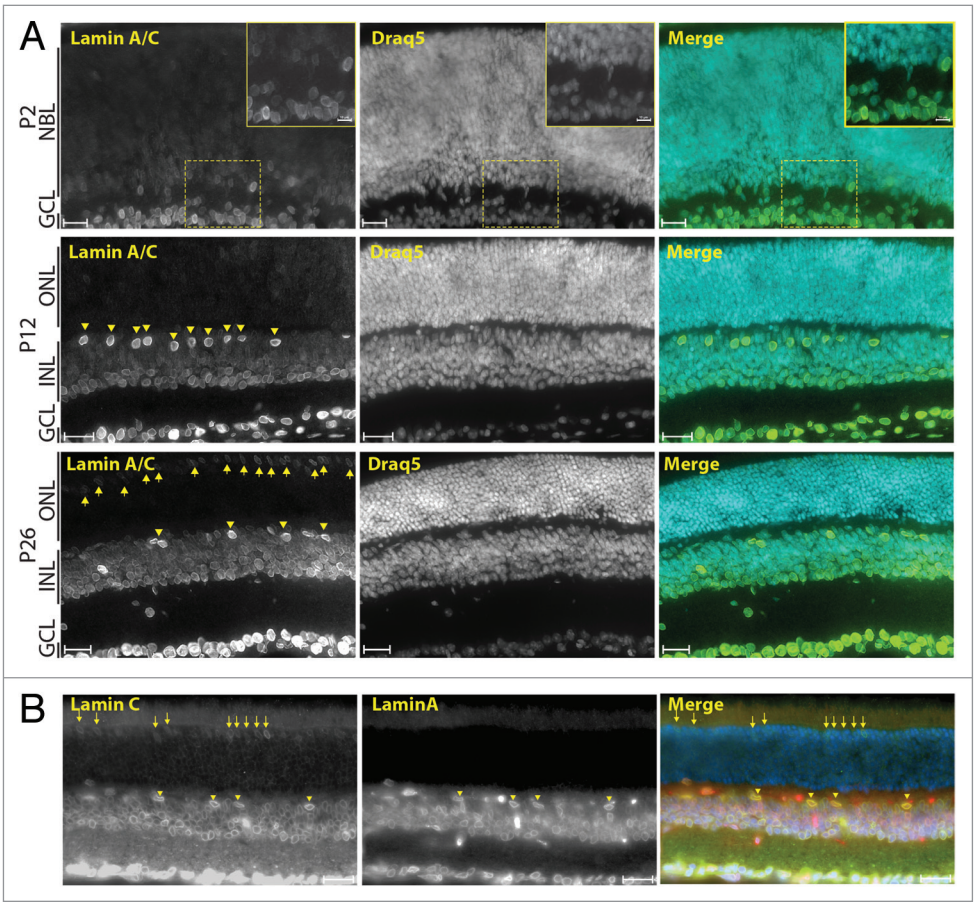

Figure 2. A-type lamins are expressed in specific post-mitotic retinal cell types. (**A**) Immunolocalization of LaminA/C in P2 (top), P12 (middle) and P26 (bottom) mouse retinas. (**B**) Coimmunolocalization of LaminA and LaminC in adult retina. Arrows point to cone photoreceptor nuclei and arrowheads to horizontal cell nuclei. Scale bars: 25 μm, insets: 10 μm.

development, we examined postnatal and adult mice retinas using antibodies against LaminA/C, LaminA, LaminC, LaminB1 and LaminB2. LaminB1 and LaminB2 were homogenously detected as typical nuclear rims in all retinal cells within P2 and P26 retinas (**Fig. 1A and B**). Interestingly, dotted patterns were also observed within the IPL and at photoreceptor synapses using two distinct antisera directed against the C-terminal region of LaminB1 (**Fig. 1A**, bottom panels and data not shown). None of these features were observed in adult retinas with the anti-LaminB2 serum (**Fig. 1B**). At P2, A-type lamins were mostly detected in a subpopulation of nuclei on the basal side of the NBL and in all GCL nuclei (**Fig. 2A**, upper panel and insets). By P12, retinal ganglion cells (RGCs, in the GCL), horizontal cells (HCs, on the apical side of the INL) and amacrine cells (ACs, on the basal side of the INL) displayed a significant enrichment of A-type lamins by comparison to other retinal neurons (**Fig. 2A**, middle panel). In adult retinas, A-type lamin expression persisted in RGCs and HCs (**Fig. 2A**) as well as in a subset of cells at the apical side of the ONL (**Fig. 2A**, lower panel). As indicated by their costaining with a cone arrestin antiserum (data not shown), these cells correspond to cone photoreceptors (CPs). Antibodies that specifically target either LaminA or LaminC were used to determine whether both isoforms are coexpressed in retinal neurons. **Figure 2B** shows that RGCs, HCs and ACs coexpressed LaminA and LaminC. By contrast, LaminC was specifically detected in CPs and a subset of bipolar cells (BCs, **Fig. 2B**). The specificity of anti A-type lamin antibodies was confirmed by the absence of any comparable signal in the ONL and INL from retina of *lmna*$^{-/-}$ mice[35] (data not shown). It is noteworthy, however, that a much reduced but reproducible nuclear rim signal was still observed in the GCL of *lmna*$^{-/-}$ retinas with these antibodies. The origin of this signal is unclear but could correspond to the residual A-type lamin protein recently reported in that mouse model.[36] Taken together, and in agreement with the developmental regulation of lamins in other tissues,[37,38] these experiments indicate that B-type lamins are ubiquitously expressed in all RPCs and post-mitotic retinal cells whereas A-type lamins expression appears to be triggered upon exit from the cell cycle in a subset of retinal cell types.

Expression pattern of Sun proteins in the developing retina. P2 and P26 retinas were stained with an affinity-purified antiserum against Sun1. Sun1 nuclear rims were detected in the NBL and RGCs in P2 retinas (**Fig. 3A**, upper panel). Expression was maintained throughout all retinal cells at P12 (not shown). In the adult retina, Sun1 expression was detected in all retinal cells but rod photoreceptors (RPs, **Fig. 3A**, lower panel). Similarly to A-type lamins (**Fig. 2A**), CPs and HCs were relatively enriched

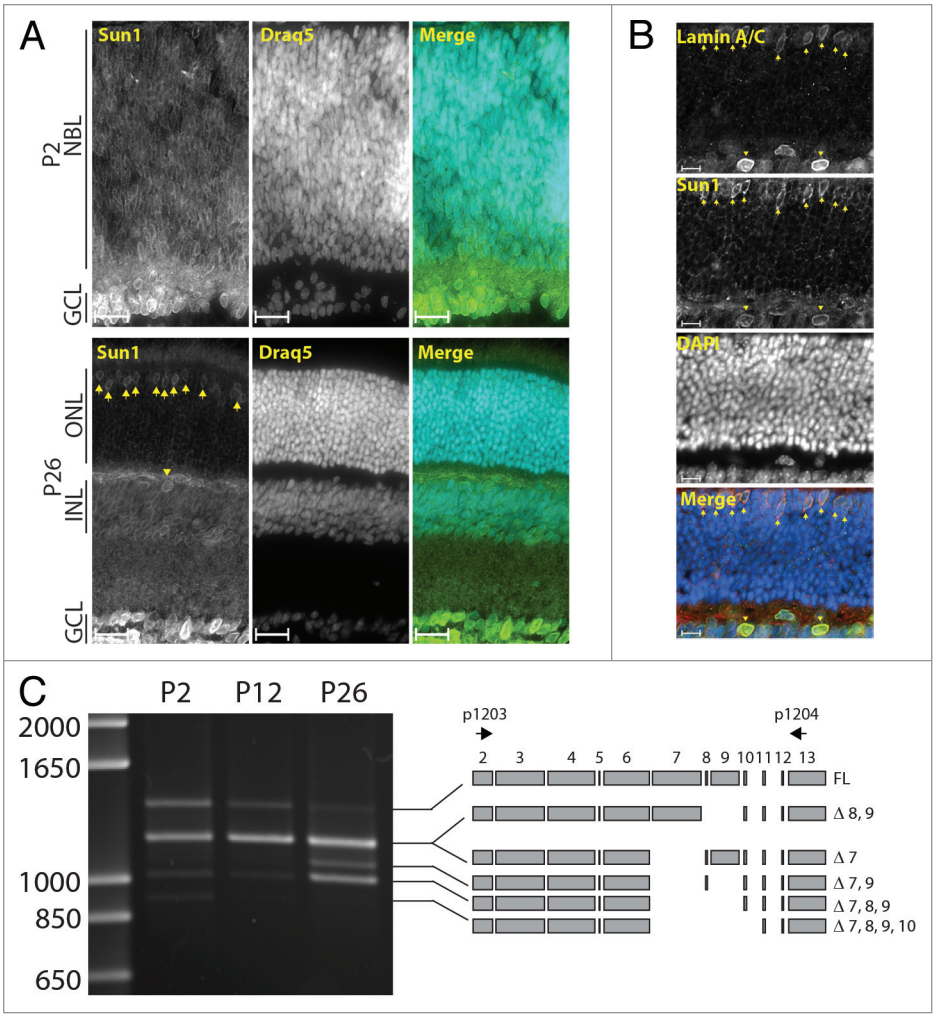

Figure 3. Expression pattern of Sun1 in the developing retina. (**A**) Immunolocalization of Sun1 in P2 (top) and P26 (bottom) retinas counterstained with DRAQ5. Scale bars: 25μm. (**B**) P26 retinas costained with LaminA/C and Sun1 and counterstained with DAPI. Scale bars: 10μm. (**C**) The alternative splicing of exons encoding the nucleoplasmic region of Sun1 is modulated during retinal development. RT-PCR of P2, P12, and P26 retina total RNA. Alternatively spliced isoforms of Sun1 transcripts and primer locations (black arrows) are depicted on the right. Cones and horizontal cells are marked with arrows and arrowheads, respectively.

in Sun1. Accordingly, both cell types could be co-stained with A-type lamin and Sun1 antisera (**Fig. 3B**). The specificity of the affinity purified anti-Sun1 antibody was verified in adult *Sun1*$^{-/-}$ mice retinas where nuclear typical Sun1 nuclear rims were absent (data not shown). The alternative splicing of a subset of exons encoding part of the nucleoplasmic region has been reported in Sun1 transcripts.[39] To determine the status of this splicing event during retinal development, a region of Sun1 encompassing exons 2–13 was amplified by RT-PCR. As shown in **Figure 3C**, a complex amplification pattern of at least six distinct alternatively spliced Sun1 transcripts was observed. Cloning and sequencing allowed for the identification of the nature of these splicing events (**Fig. 3C**). At P2, the predominant transcripts were represented by FL, Δ7 and Δ8,9. Note that because Δ7 and Δ8,9 amplicons differs by only 15 bp (767 bp and 782 bp, respectively), they are indistinguishable by gel electrophoresis. Interestingly, whereas the intensity of the Δ7 and Δ8,9 bands remained roughly constant during retinal development, the abundance of FL transcripts progressively decreased. This decrease was accompanied by a significant increase in Δ7,9 and Δ7,8,9 transcripts. These results indicate that splicing of the nucleoplasmic domain of Sun1 is developmentally regulated during retinogenesis and that the expression of spliced isoforms of Sun1 transcripts prevails in the adult retina.

Whereas Sun1 expression was detected during early postnatal retinal development and in all retinal cells but RPs, Sun2 expression appeared more restricted. Faint Sun2 nuclear rims were detected in RGCs at P2 and P12 (not shown). In adult retinas, Sun2 was strongly expressed in RGCs, in ACs on the basal side of the INL and to a lesser extent in CPs (**Fig. 4A**). Because Sun2 could not be detected in the NBL using IF, we performed in situ hybridization (ISH) using Sun2 specific probes (**Fig. 4B**). Sun2 transcripts were clearly detected in the NBL at P2. At P12, Sun2 transcripts were mostly detected in the INL and to a lesser extent within the developing ONL. In adult retina, Sun2 mRNA was mostly detected in the INL as well as in a few sparse cells of the ONL that may correspond to the weak Sun2 rims observed in IF in CPs (**Fig. 4A**).

Because of the complexity of the alternative splicing of the nucleoplasmic region of Sun1, we also examined the alternative splicing status of exons encoding the nucleoplasmic region of Sun2. Except for the alternative splicing of exon5, Sun2 transcripts were represented by the full assortment of exons encoding its nucleoplasmic region (**Fig. 4C**).

Together, these results indicate that Sun1 and Sun2 are differentially expressed in adult retinal cell populations and that the nucleoplasmic region of Sun1 displays a relatively complex alternative splicing pattern relative to Sun2.

Expression of nesprins in the developing retina. To characterize the expression of nesprins during retinal development, a new antiserum was raised against an 882-amino-acid epitope located just upstream the KASH domain (residues 2047 to 2928 of RefSeq NP_ 001073154.1) and encompassing the five C-terminal spectrin repeats of nesprin1 (see Materials and Methods). This antiserum did not display any clear NE staining at P2 (data not shown). In P26 retinas, nuclear rims could be observed in the GCL and the INL (**Fig. 5A**). ISH using probes designed against

the C-terminal region of nesprin1 (ENSMUST00000056571 region 20 000–26 000) revealed that only basalmost cells of the NBL and most cells of the GCL were stained at P2 (**Fig. 5B**). In P12, nesprin1 mRNA labeling increased within the INL and the GCL whereas spare dots were detected in the ONL (**Fig. 5B**). In adult retinas, we observed a very dense signal both in the INL and GCL. In the former, several "hot spots" were observed on both the inner and outer edges of adult INL suggesting high expression levels of nesprin1 in specific retinal subpopulations.

In an attempt to identify nesprin1 isoform(s) potentially accounting for the mRNA induction observed in ISH, the anti-nesprin1 serum was used to perform immunoblots on P2, P12 and P26 retina lysates (**Fig. 5C**). Whereas high molecular weight bands migrating at ~250 kDa were detected at all time-points, P2 retinas specifically displayed immunoreactive bands of higher molecular weight. Interestingly, the expression of a ~120 kDa immunoreactive band was strongly induced in adult retinas (**Fig. 5C**). Immunoprecipitation followed by mass spectrometry identification of its tryptic peptides identified that band as nesprin1α (Reference protein NP_071310.2), a nesprin1 isoform of 949 amino acids (predicted MW of 109 kDa) that harbors five spectrin repeats (**Fig. 5D**).

A recent study showed that the second to last exon of nesprin1 transcripts is alternatively spliced in adult mouse brain, an event that may potentially lead to the synthesis of KASH-less isoforms of nesprin1.[40] To determine if such alternative splicing takes place in the retina, RT-PCR reactions were performed on total RNA extracted from P2, P12 and P26 retinas using primers hybridizing within the last and third to last exons of nesprin1.[40] Two distinct bands were amplified in RT-PCR (**Fig. 5E**). In agreement with the paucity of nesprin1 signal observed in ISH at P2 (**Fig. 5B**), RT-PCR products amplified from P2 retina were significantly less abundant than at P12 and P26. Cloning and DNA sequencing confirmed the alternative splicing of the penultimate exon of nesprin1 transcripts (**Fig. 5E**). This splicing event results in the early termination of the nesprin1 ORF to produce a putative KASH-less isoform of nesprin1 with an alternative C-terminal primary sequence (**Fig. 5D**). RT-PCR amplifications performed with the same primers on total RNA from various mouse tissues further indicated that the alternative splicing of the penultimate exon of nesprin1 is significantly more abundant in CNS tissues (**Fig. 5F**). Indeed, the typical doublet was observed to a greater extent in brain, cerebellum and retina whereas the unspliced nesprin1 transcript was largely predominant in heart, skeletal muscle, liver and small intestine. Interestingly, in brain and cerebellum, the spliced transcript was relatively more abundant than the unspliced one thereby suggesting that KASH-less isoform(s) of nesprin1 are abundantly expressed in these tissues.

To analyze nesprin2, we used an antiserum whose epitope corresponds to 427 amino acids encompassing the two C-terminal spectrin repeats of nesprin just upstream of the KASH domain (residues 6354 to 6780 of RefSeq NP_001005510.2). In stark contrast with nesprin1, nesprin2 nuclear rims were detected in the NBL of P2 retinas (**Fig. 6A**, top panel). That observation was further corroborated by positive ISH within the NBL using probes targeting bases 15 000 to 20 000 of nesprin2 mRNA (NM_001005510.2),

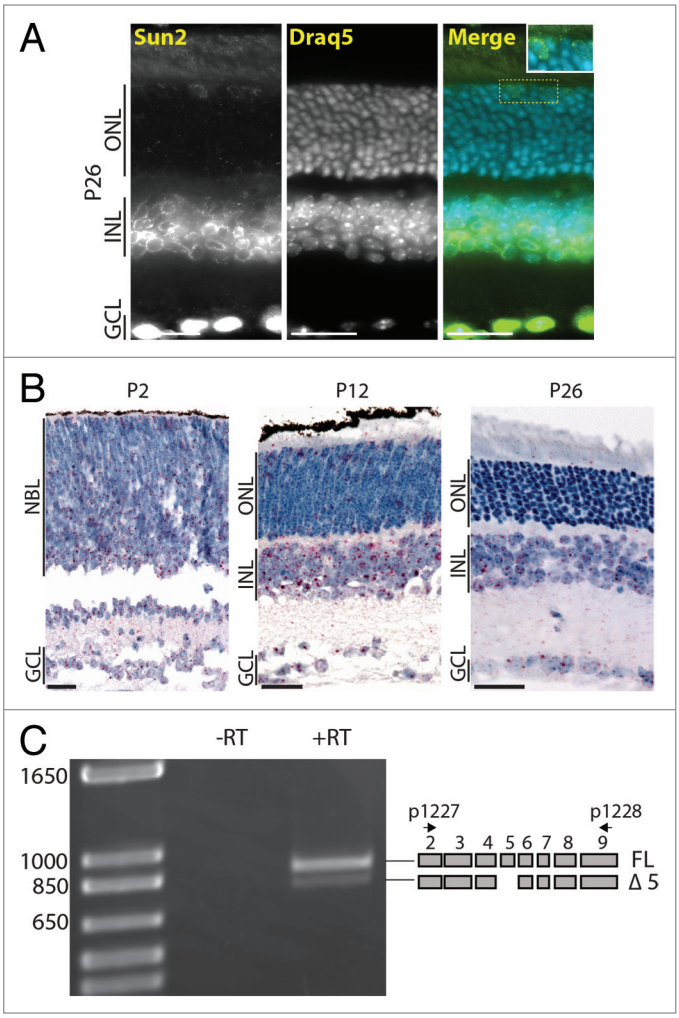

Figure 4. Expression pattern of Sun2 in the developing retina. (**A**) Typical Sun2 immunostaining pattern of RGC, amacrine and cones nuclei in P26 retina. Scale bars: 25μm, 5μm in inset. (**B**) In situ hybridization of P2 (left), P12 (middle) and P26 (right) retinas. Scale bars: 25μm. (**C**) Exon5, encoding a stretch of the nucleoplasmic region of Sun2, is alternatively spliced in retina.

a region that encodes the C-terminal end of the protein (**Fig. 6B**, left panel). In adult retinas, nesprin2 expression at the NE was detectable in the GCL and a subset of nuclei in the basal half of the INL (presumably ACs) but was absent in the ONL (**Fig. 6A**, lower panel). Western blots of P2, P12 and P26 lysates revealed that P2 retinas revealed the presence of high molecular weight immunoreactive nesprin2 bands that were subsequently downregulated in P12 and P26 retinas (**Fig. 6C**). These high molecular weight proteins most likely include the giant isoforms of nesprin2.[41,42] Bands whose size ranged from 150 kDa up until the molecular weight of the giant isoform may either correspond to specific nesprin2 isoforms of intermediate molecular weight or to degradation products of the giant isoform.[41,42] Interestingly, whereas a significant amount of nesprin2 mRNA was detected in the inner segment of the photoreceptor layer in ISH (**Fig. 6B**, middle and right panels), we could not detect any nesprin2 nuclear rims within adult ONL (**Fig. 6A**, lower panel) suggesting that these transcripts may

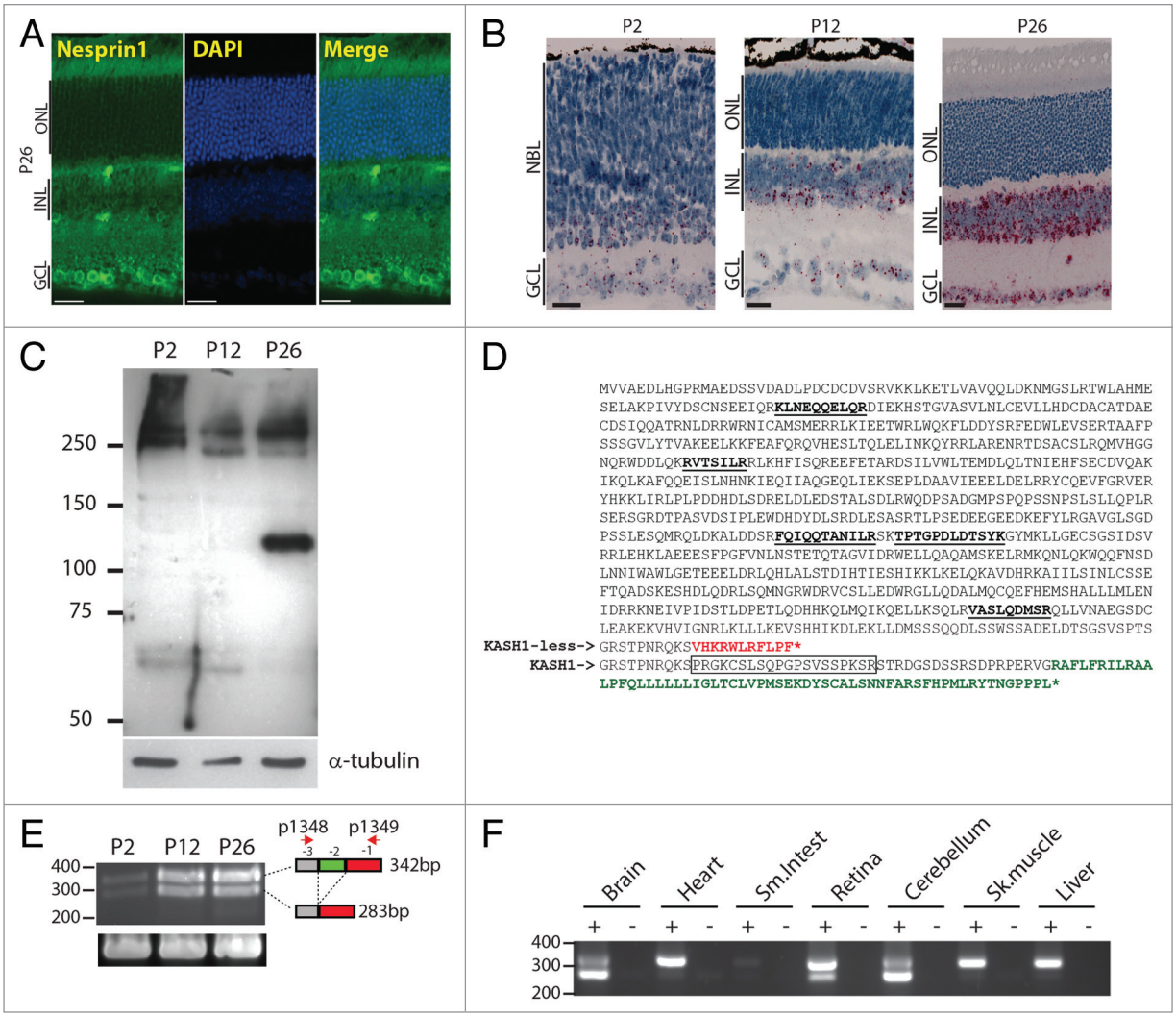

Figure 5. Expression pattern of nesprin1 in the developing retina. (**A**) Immunolocalization of nesprin1 in P26 retinas counterstained with DAPI. Scale bars: 25μm. (**B**) In situ hybridization of P2 (left), P12 (middle) and P26 (right) mouse retinas using probes recognizing the C-terminal region of nesprin1 mRNA. Scale bars: 25μm. (**C**) Immunobloting of P2, P12 and P26 retina lysates with an anti-nesprin1 antibody. Note the induction of a ~120 kDa nesprin1 species, identified as nesprin1α, in P26 retinas. Alpha-tubulin was used to control for comparable loading. (**D**) Primary sequence of nesprin1α whose expression is induced in adult retina. Tryptic peptides identified by mass spectrometry are underlined. The primary sequence of the KASH domain is in green. Amino acids encoded by the penultimate exon (-2) of nesprin1 is boxed. The alternative C-terminal stretch of amino acids of KASH-less nesprin1 is in red. (**E**) Identification of transcripts encoding KASH-less nesprin1. RT-PCR on total RNA extracted from P2, P12, and P26 retinas. GAPDH was used as a control for amplified RNA amount. Splicing of the penultimate exon (-2) predicts the amplification of a 283 bp product rather than the canonical 342 bp. (**F**) Same experiment as in (**E**) performed on total RNA extracted from different mouse tissues.

encode nesprin2 isoforms devoid of KASH domains. Transcripts encoding KASH-less isoforms of nesprin2 were recently shown to be generated either through alternative splicing of exon 111/112 or through the alternative polyadenylation of nesprin2 transcripts.[42] To examine alternative splicing, RT-PCR amplifications were performed with primers p1380 and p1381 using total RNA from different mouse tissues (**Fig. 6D and G**). A single band was amplified from all tissues and contained all but exon114. RT-PCR amplification of a larger amplicon (primers p1266/p1381, **Fig. 6E and G**) also produced a single band containing all but exon114. Because the absence of exon 114 does not alter the reading frame of the nesprin2 gene, we conclude that, by contrast to nesprin1, exons encoding the C-terminal region of nesprin2 are not subject to alternative splicing in the retina. To examine the possibility that alternative polyadenylation may underlie the synthesis of KASH-less isoform of nesprin2, 3' RACE PCR was performed using primers p1380 in conjunction with a reverse anchor primer (see Materials and Methods). A strong band of ~1200 bp was amplified and contained the whole 3' UTR encoded by exon 116 preceded by all but exon 114. Weaker bands at ~200, 300, and 400 bp (asterisks, **Fig. 6F**) corresponded to non-specific amplifications products resulting from primers misannealing in this less stringent PCR approach.

Taken together, our data indicate that nesprin1 and 2 both undergo marked shifts in the expression pattern of their respective isoforms during retinal development and that their spatiotemporal

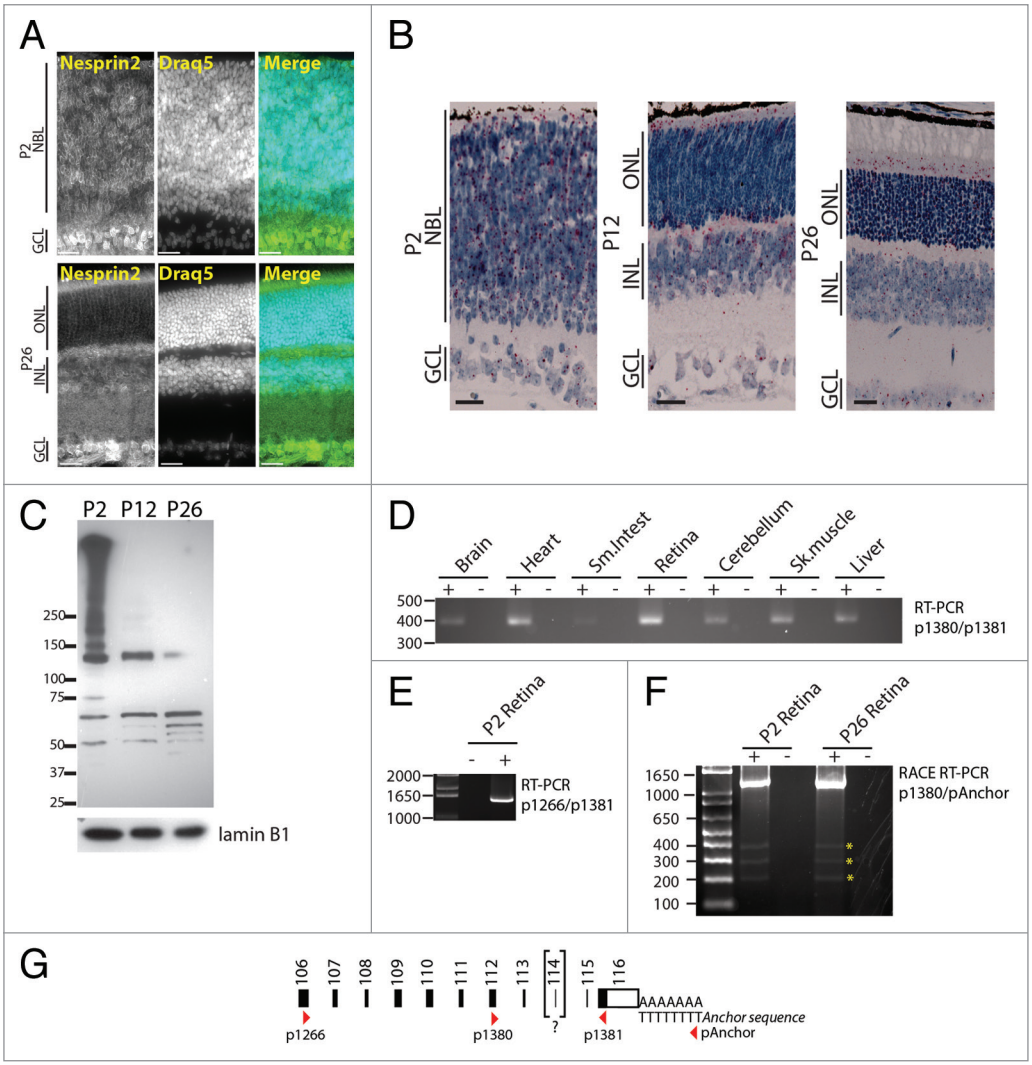

Figure 6. Expression pattern of nesprin2 in the developing retina. (**A**) P2 (top) and P26 (bottom) retinas were stained with an affinity purified nesprin2 antibody and counterstained with DRAQ5. Note the homogenous expression of nesprin2 in the NBL of P2 retinas. Scale bars: 25μm. (**B**) In situ hybridization on P2 (top), P12 (middle), and P26 (bottom) retinas using probes recognizing the C-terminal region of nesprin2 mRNA. Scale bars: 25μm. (**C**) Immunoblotting of P2, P12, and P26 retina lysates with an affinity purified anti-nesprin2 antiserum. Note the downregulation of multiple high molecular weight bands as retinogenesis proceeds. LaminB1 was used to control for comparable loading. (**D**) RT-PCR amplification of nesprin2 transcripts from total RNA extracted from the indicated mouse tissues using the p1380/p1381 primer pair. (**E**) Same experiment as in (**D**) with the p1266/p1381 primer pair on retina total RNA. (**F**) 3′RACE RT-PCR performed on total RNA extracted from P2 and P26 retina using the p1380 specific forward primer and the reverse pAnchor primer. Asterisks denote non-specific amplified bands. (**G**) Localization of primers used in PCR reactions relative to the C-terminal exons of nesprin2 transcripts. Bracketing of exon 114 reflects its absence in all amplicons sequenced in this study.

expression patterns are significantly different. Indeed, whereas nesprin2 transcripts or nuclear rims could be detected in the NBL of P2 retinas using ISH and IF, nesprin1 expression in progenitor cells could not be detected using either technique. Finally, whereas our data strongly suggest that KASH-less isoforms of nesprin1 is a significant output of the nesprin1 gene, we were unable to identify any nesprin2 transcript that would encode KASH-less isoforms of nesprin2 in the retina.

Discussion

In the present study, we performed immunofluorescence microscopy, in situ hybridization, immunoblotting and PCR amplifications to get more insight into the composition of LINC complexes during postnatal retinal development. Whereas each technique has its own advantages, they also come with their own drawbacks. For example, immunofluorescence microscopy allows for excellent spatial localization of an epitope but the complete absence of any significant signal does not permit us to formally conclude that this epitope is not expressed. In situ hybridization, on the other hand, allows for more reliable target recognition but lacks the spatial precision offered by IF. Finally, immunoreactive species detected in immunobloting of dissected retina may originate either from the neuroretina or from the retinal vasculature. Keeping these limitations in mind, the combination of these complementary approaches allowed us to draw several important

conclusions related to the composition of LINC complexes at different time points of postnatal retinal development.

Lamins form a meshwork of type-V intermediate filaments that line the nucleoplasmic side of the INM. Here, in agreement with previous studies,[43,44] we observed that B-type lamins are homogenously expressed in retinal progenitor cells and later in all differentiated retinal cell types. By contrast, and in agreement with recent studies,[45,46] A-type lamins are expressed at various levels and exclusively in post-mitotic cells. B-type lamins, rather than A-type lamins, are therefore more likely to play a role in CNS development. Accordingly, *lmnb1*$^{-/-}$ and *lmnb2*$^{-/-}$ mice display severe CNS developmental defects and die at birth whereas *lmna*$^{-/-}$ mice are normal and indistinguishable from their heterozygous littermates at birth.[35] Interestingly, using two distinct anti-LaminB1 antibodies on WT retinas, we observed a dotted pattern that roughly delineated the stratified synaptic zones of bipolar cells within the IPL and the photoreceptor synapses on the apical side of the OPL. Because LaminB2 immunoreactive species were recently identified in mitochondria of RGC axonal synapses,[47] further studies are needed to determine whether these dotted patterns in the retina correspond to potential non-canonical variant of LaminB1. In agreement with recent reports in rat and mouse retina,[45,46] we found that the expression of A-type lamins is heterogeneous and variable in different neuronal types of adult retina. We further expand upon these findings by showing that the expression of A-type Lamins is regulated in a spatio-temporal manner in the mouse retina. Indeed, HCs and RGCs express high levels of A-type lamins throughout retinal development. Furthermore, CPs could be distinguished from rods through A-type lamins expression. Antibodies specific for either LaminA or LaminC further indicated that RGCs, HCs and ACs coexpress these isoforms whereas CPs specifically express LaminC. Whereas we previously showed that LINC complexes are essential for the proper localization of cone nuclei on the apical side of adult retinas,[13] the expression of A-type lamins was dispensable. Hence, the expression of LaminC is most likely not involved in cone nuclei positioning.

Similarly to B-type lamins, Sun1-positive nuclear rims were detected early in retinogenesis within all cells of the NBL and developing GCL. By contrast, Sun1 expression pattern more closely resembled the expression pattern of A-type lamins in adult retinas where Sun1 antibodies also preferentially decorated the NE of CPs, HCs and RGCs. Interestingly, we observed that exons 7 to 10, which encode the central part of the nucleoplasmic region of Sun1, are alternatively spliced and that this splicing appears to be modulated during retinal development. Because Sun1 isoforms putatively encoded by these transcript variants are difficult to resolve in western blot, their synthesis remains to be formally demonstrated. However, Sun1 enrichment in CPs, HCs, and RGCs of adult retina raises the intriguing possibility that individual Sun1 isoforms may fulfill cell-specific physiological roles. This concept is indeed supported by the recent identification of a Sun1 variant (Δ5–10) that is exclusively expressed in spermatids where it plays a role in sperm head formation and by the cell type-specific expression of different variants of Sun1 isoforms.[39,48] At P2, we could not detect any Sun2 rims within the NBL in immunofluorescence microscopy. This observation contrasts with ISH results that clearly emphasized the presence of Sun2 transcripts across the NBL. In addition, because Yu et al. were able to detect Sun2 within the NBL,[14] either our Sun2 antiserum may not efficiently recognize Sun2 in the NBL or it may recognize a different isoform that is not yet expressed during early retinogenesis. In adult retinas, Sun2 could be detected within RGCs and to a lesser extent in CPs and cells located on the basal side on the INL (most likely ACs). ISH on P26 retina was in agreement with IF results.

Nesprin2 mRNA expression and localization at the NE of NBL cells could readily be detected in P2 retina. By contrast, neither nesprin1 mRNA expression nor nesprin1 protein expression at the NE could be detected in the NBL of P2 retina. These results, in addition with similar IF findings reported by Yu et al. using with different nesprin antibodies,[14] strongly suggest that nesprin1 and nesprin2 display very distinct spatiotemporal expression patterns in CNS tissues. Immunoblots experiments revealed the presence of high molecular weight isoforms of nesprin2 in P2 retina lysates. These isoforms are subsequently downregulated as retinogenesis proceeds. Because most retinal cell types have reached their final laminar position by P12, our results collectively suggest that high molecular weight isoforms of nesprin2 interact with Sun1 to enable nuclear movements associated to early phases of retinal development. Accordingly, retina from nesprin2 and Sun1 KO mice display early developmental defects leading to abnormal morphological features and electroretinogram recordings in adult mice.[14]

In adult retina, we observed a major upregulation of nesprin1 transcripts within the INL and the GCL at later stages of retinal development. We currently hypothesize that this induction corresponds to the spike of nesprin1α expression we observed in immunoblots late in neurogenesis. No comparable induction of a specific nesprin2 isoforms could be detected either by immunoblot or ISH late in neurogenesis. This set of results indicate that retinogenesis is characterized by a shift in the qualitative expression pattern of nesprin1 and 2 isoforms. This is similar to findings reported by Randles et al. during skeletal muscle development.[49]

Interestingly, despite the detection of nesprin transcripts in the ONL of adult retinas by ISH, we could not detect any nesprin nuclear rim in either CPs or RPs even though such rims were detected in other populations of adult retinal cells. Rather, we reproducibly observed a significant signal in the inner segment of photoreceptors using either nesprin1 or 2 antibodies. Importantly, similar observations were reported by Yu et al. using distinct anti-nesprin1 antibodies.[14] Because transcripts that potentially encode KASH-less isoforms of nesprins have recently been reported,[42,50] the absence of nesprin rims in CPs and RPs could be explained by the synthesis of KASH-less isoforms of nesprins in the photoreceptor layer. Because they lack the KASH domains, such isoforms would be unable to localize to the NE. KASH-less encoding transcripts of nesprin1 were indeed detected in the retina and database searches further indicated that this splicing is present in polyadenylated nesprin1 mRNAs isolated from a C57/BL6 retina library (cDNA clone IMAGE: 5366479, GenBank accession# BC110426.1). Taken together, these results provide evidence that KASH-less isoforms of nesprin1 are synthesized at

least in photoreceptors where they may play a physiological role beyond the NE. It is possible that this alternative splicing leading to the synthesis of KASH-less isoforms of nesprins may be evolutionary conserved; indeed, similar alternative splicing events of Klar, a *D. melanogaster* nesprin ortholog, lead to the synthesis of a KASH-less isoform thereof.[51] This isoform (Klarβ) mediates embryonic lipid droplets movement by contrast to KASH-containing isoforms (Klarα) that mediate photoreceptor nuclear movements.[31,51,52]

We found that the splicing of the penultimate exon of nesprin1 transcripts is much more frequent in retina, brain and cerebellum than in non-CNS tissues further suggesting that KASH-less isoforms of nesprin1 play important roles in CNS tissues. In humans, mutations of nesprin1 are linked to autosomal recessive cerebellar ataxia type1 (ARCA1).[53] Hence, the molecular etiology of this pathology could potentially originate from the effect these mutations have on the physiological function that KASH-less isoforms of nesprin1 may perform in the cerebellum. Because nesprins contain multiple spectrin repeats and recombinant KASH-less nesprin1 isoforms localize to the nuclear matrix and cytoplasm of transfected cells,[42] a structural role for KASH-less isoforms in the cerebellum may be envisioned. For these reasons, whereas we have now learned a lot about the physiological function of nesprin1 in the context of LINC complexes, more studies are needed to understand the role of KASH-less isoforms of nesprin1 in CNS tissues. Using both RT-PCR and 3'RACE-PCR, we were unable to identify any transcript that may encode a KASH-less isoform of nesprin2 in the retina even though such isoforms have readily been detected through either alternative splicing of exons 111/112 or alternative polyadenylation in other tissues or cells.[42] We only found that exon114 was missing from all nesprin2 amplicons, an event that does not alter nesprin2 transcripts reading frames.

In summary, our results indicate that in RPCs, LINC complexes are mostly composed of B-type lamins, Sun1, and nesprin2 where Sun1 may be represented by different isoforms harboring distinct nucleoplasmic regions and nesprin2 by high molecular weight isoforms that are downregulated as retinogenesis proceeds. By contrast, the composition of LINC complexes varies in a cell type-specific manner within postmitotic retinal cells. Purified retinal neuroblasts should further pinpoint the identity of Sun1 and nesprin2 isoforms. Because Sun1 and nesprin2 gene products are involved in IKNM in mouse retina,[14] future studies aimed at the identification Sun1 and nesprin2 isoforms expressed in RPC is likely to provide novel insights in mechanistic aspects underlying IKNM.

Materials and Methods

Mice. Animal protocols used in this study adhered to the ethical and sensitive care and use of animals in research and were approved by the Washington University School of Medicine Animal Studies Committee (Animal Welfare Assurance Permit # A-3381-01, protocol # 20110163). *lmna*$^{+/-}$ mice (B6.1291S1(Cg)-LMNA^{tm1Stw}/BkknJ, #009125) and *Sun1*$^{+/-}$ mice (B6;129S6-Sun1^{tm1Mhan}/J, #012715) were purchased from The Jackson Laboratory.[35,54] Mouse colonies were maintained and genotyped at the Mouse Genetics Core (Washington University School of Medicine).

Preparation of mouse retinas. Mice were sacrificed via CO_2 inhalation and ocular globes were immediately isolated and rinsed in PBS. Several incisions were performed in the cornea before incubating the whole eye in 4% paraformaldehyde (PFA)/PBS for 1 h at 4°C, rinsed in PBS, incubated overnight in a 30% sucrose/PBS solution and embedded in OCT compound (Tissue-TEK, #4583). For immunofluorescence microscopy, cryosections (15 μm) on Superfrost Plus slides (VWR) were fixed for 10 min in 2.5% PFA in PBS, rinsed three times in PBS, permeabilized in 0.5% Triton X-100/PBS and incubated with primary antibodies diluted in 10% goat or donkey serum/0.5% Triton X-100 in PBS. Alexa-conjugated secondary antibodies (Invitrogen) were incubated in the same conditions. Following DAPI/DRAQ5 staining, slices were mounted in fluorescent mounting medium (DAKO, #S3023). Tiled images were acquired on an Eclipse Ti inverted fluorescence microscope (Nikon, Melville, NY, USA) controlled by NIS Elements software using either 20× or 40× objectives and a CoolSnap HQ_2 camera (Photometrics).

Antibodies. Anti-LaminB2 (Invitrogen, #332100), anti-LaminA/C (Santa Cruz Biotechnology, #SC-6215), anti-LaminB1 (Santa Cruz Biotechnology, #SC-6210), anti-cone arrestin (Millipore, #AB15282), anti-Calbindin (Sigma, #C9848 and Cell Signaling, #2173), were used in this study. Affinity purified- anti-mouse nesprin2, anti-human LaminC and anti-mouse Sun2 were previously described.[55-57] To generate the affinity purified anti-mouse Sun1 antibody, total RNA of C2C12 cells was reverse transcribed and PCR amplified using primers pairs annealing to exons 13 and 18. PCR products were cloned into the pcr8 gw Topo vector (Invitrogen) and sequenced. LR clonase reactions were performed according to the manufacturer's protocol (Invitrogen) to obtain an N-terminal GST fusion protein. Bacterial synthesis of recombinant protein was induced using IPTG in BL21 *E. coli* and proteins were extracted from inclusion bodies in urea. Samples were separated on a superdex200 column (GE Healthcare) and concentrated using an Amicon Ultracell 10k. Polyclonal antibodies were produced by immunizing rabbits with the purified GST fusion proteins and affinity-purified on a CNBr sepharose column (PRIMM Biotech). The anti-nesprin1 antibody was produced against an 882 amino acid recombinant fusion protein located just upstream of the KASH-domain using the same procedure as described above (no affinity purification was performed). The monoclonal anti LaminA antibody was generated against a synthetic peptide corresponding to amino acids 570–588 (CSSSGDPAEY NLRSRTVLC) of human LaminA and affinity purified. HRP- and Alexa-conjugated secondary antibodies were obtained from Santa Cruz Biotechnology and Invitrogen, respectively.

RNA extraction and transcripts analyses. Mouse tissues were isolated and resuspended in Trizol (Invitrogen, #15596020), grinded with a Bullet Blender (Next Advance) and centrifuged. The supernatants were then used for RNA purification according to the manufacturer's specifications. One microgram of total RNA was reverse transcribed with Superscript II (Invitrogen, #18064014)

following manufacturer recommendations. Ten percent of RT reactions was used with Taq Hi-FI polymerase (Invitrogen, 11304-011). Thirty amplification cycles were performed using primers p1203 (ATGGACTTTT CTCGGCTGCA CACG) and p1204 (TCTATGCATG CCCTTGGAAT CGTCCAC) for Sun1, p1227 (5'-GCGCCTCACT CGCTACTCTC AGGATGATAA CG-3') and p1228 (5'-GGAGGAAAAG TCTGCAGCAA GGGCTTCC-3') for Sun2, p1348 (5'-GTCCCACATC CGGAAGAAGT ACCCC-3') and p1349(5'-CTTCAGAGTG GAGGACCGTT GG-3') for nesprin1, p1266(5'-ATGATAGAAG ACCCCAGGGA GATCCAGGCT GAC-3'), P1380(5'-GCAAGAGCAA GTGGCTCAAG ATCTGATGTC CTTGC-3'), P1381(5'-CTAGGTGGGA GGTGGCCCGT TGGTGTAC-3') for nesprin2. 3' RACE-PCR was performed according to the manufacturer recommendation (Roche, 5'/3' RACE kit 2nd generation, #03353621001) using an oligo-dT fused to an anchor sequence for the reverse transcription reaction. For the PCR amplification step, a forward primer specific to either nesprin1 or 2 was used in conjunction with the reverse anchor primer provided with the kit. Ethidium bromide-stained agarose gels were imaged with a G:Box HR16 imaging system (Syngene). Sequencing reactions were performed at our in-house facility (Protein and Nucleic Acid Chemistry Laboratory, Washington University School of Medicine).

Western blotting. Retinas were isolated and resuspended and boiled in laemli buffer supplemented with 8M urea. Proteins were separated by SDS-PAGE and transferred to Optitran nitrocellulose membranes (GE Healthcare). Membranes were blocked with 5% milk in TBST for 1 h at room temperature and incubated overnight at 4 °C with the appropriate affinity purified antibodies. After washing with TBST, membranes were incubated with an HRP-conjugated secondary antibodies. Signals were detected using SuperSignal® West Pico solutions (Thermo, #1856135) and exposed on X-ray film. Films were digitized using a G:Box HR16 imaging system (Syngene).

In situ hybridization. ISH was performed on mouse eye sections using the RNAscope 2.0 Red Kit (Advanced Cell Diagnostics, #310036) according to the manufacturer's instructions. Briefly, sections were deparaffinized in xylene, followed by dehydration in an ethanol series. Sections were then incubated in a boiling citrate buffer, rinsed with water and immediately treated with protease. Hybridization with target probes, preamplifier and amplifier were performed at 40 °C followed by development using the supplied Fast Red reagents. Control hybridizations with non-specific probes were performed in parallel with all test hybridization. Samples were couterstained with Hematoxylin and tiled images were acquired on a DM5500 (Leica) upright light microscope fitted with a DFC295 color camera and a 40× objective.

Immunoprecipitation and mass spectrometry. Retinas were isolated and resuspended in RIPA buffer (150 mM NaCl, 50 mM Tris pH 7.6, 0.5% Sodium Deoxycholate, 0.1% SDS, 1% Triton X-100) with protease inhibitors (Roche, #11697498001). Lysates were pre-cleared for at least 1 h by incubating post pellet supernatants with Protein A/G beads (Pierce, #20421) and the corresponding naïve IgG. Cleared supernatants were then incubated with fresh Protein A/G and immunoprecipitating antibody on a rotary shaker overnight at 4 °C. Beads were washed three times with RIPA buffer and resuspended in laemli buffer. Silver staining was performed according to the manufacturer recommendation (Invitrogen, #LC6070) on 20% of immunoprecipitation reactions. Tryptic digests and Mass spectrometry analyses were performed at the Donald Danforth Plant Sciences Center Proteomics and Mass Spectrometry Facility.

Disclosure of Potential Conflicts of Interest

No potential conflict of interest was disclosed.

Acknowledgments

We thank the staff of the Mouse Genetics Core and of the Morphology and Imaging Core at Washington University School of Medicine as well as Dr Min Han for the kind gift of the anti-mouse Sun2 antibody. This work was supported by the National Institute of Health (EY022632 to Hodzic D), an NIH Training Grant (T32 EY013360 to Razafsky DS), the McDonnell Center for Cellular and Molecular Neurobiology at Washington University School of Medicine (to Hodzik D) and by awards to the Department of Ophthalmology and Visual Sciences at Washington University from a Research to Prevent Blindness, Inc. Unrestricted grant and the NIH vision Core Grant (P30 EY002687).

References

1. Baye LM, Link BA. Nuclear migration during retinal development. Brain Res 2008; 1192:29-36; PMID:17560964; http://dx.doi.org/10.1016/j.brainres.2007.05.021
2. Swaroop A, Kim D, Forrest D. Transcriptional regulation of photoreceptor development and homeostasis in the mammalian retina. Nat Rev Neurosci 2010; 11:563-76; PMID:20648062; http://dx.doi.org/10.1038/nrn2880
3. Miyata T. Development of three-dimensional architecture of the neuroepithelium: role of pseudostratification and cellular 'community'. Dev Growth Differ 2008; 50(Suppl 1):S105-12; PMID:18070110; http://dx.doi.org/10.1111/j.1440-169X.2007.00980.x
4. Spear PC, Erickson CA. Interkinetic nuclear migration: a mysterious process in search of a function. Dev Growth Differ 2012; 54:306-16; PMID:22524603; http://dx.doi.org/10.1111/j.1440-169X.2012.01342.x
5. Kosodo Y. Interkinetic nuclear migration: beyond a hallmark of neurogenesis. Cell Mol Life Sci 2012; 69:2727-38; PMID:22415322; http://dx.doi.org/10.1007/s00018-012-0952-2
6. Ghashghaei HT, Lai C, Anton ES. Neuronal migration in the adult brain: are we there yet? Nat Rev Neurosci 2007; 8:141-51; PMID:17237805; http://dx.doi.org/10.1038/nrn2074
7. Kato M, Dobyns WB. Lissencephaly and the molecular basis of neuronal migration. Hum Mol Genet 2003; 12(Spec No 1):R89-96; PMID:12668601; http://dx.doi.org/10.1093/hmg/ddg086
8. Nabi NU, Mezer E, Blaser SI, Levin AA, Buncic JR. Ocular findings in lissencephaly. J AAPOS 2003; 7:178-84; PMID:12825057; http://dx.doi.org/10.1016/S1091-8531(02)42005-8
9. Rich KA, Zhan Y, Blanks JC. Migration and synaptogenesis of cone photoreceptors in the developing mouse retina. J Comp Neurol 1997; 388:47-63; PMID:9364238; http://dx.doi.org/10.1002/(SICI)1096-9861(19971110)388:1<47::AID-CNE4>3.0.CO;2-O
10. Poché RA, Reese BE. Retinal horizontal cells: challenging paradigms of neural development and cancer biology. Development 2009; 136:2141-51; PMID:19502480; http://dx.doi.org/10.1242/dev.033175
11. Poché RA, Kwan KM, Raven MA, Furuta Y, Reese BE, Behringer RR. Lim1 is essential for the correct laminar positioning of retinal horizontal cells. J Neurosci 2007; 27:14099-107; PMID:18094249; http://dx.doi.org/10.1523/JNEUROSCI.4046-07.2007
12. Edqvist PH, Hallböök F. Newborn horizontal cells migrate bi-directionally across the neuroepithelium during retinal development. Development 2004; 131:1343-51; PMID:14973293; http://dx.doi.org/10.1242/dev.01018
13. Razafsky D, Blecher N, Markov A, Stewart-Hutchinson PJ, Hodzic D. LINC complexes mediate the positioning of cone photoreceptor nuclei in mouse retina. PLoS One 2012; 7:e47180; PMID:23071752; http://dx.doi.org/10.1371/journal.pone.0047180

14. Yu J, Lei K, Zhou M, Craft CM, Xu G, Xu T, Zhuang Y, Xu R, Han M. KASH protein Syne-2/Nesprin-2 and SUN proteins SUN1/2 mediate nuclear migration during mammalian retinal development. Hum Mol Genet 2011; 20:1061-73; PMID:21177258; http://dx.doi.org/10.1093/hmg/ddq549
15. Zhang X, Lei K, Yuan X, Wu X, Zhuang Y, Xu T, Xu R, Han M. SUN1/2 and Syne/Nesprin-1/2 complexes connect centrosome to the nucleus during neurogenesis and neuronal migration in mice. Neuron 2009; 64:173-87; PMID:19874786; http://dx.doi.org/10.1016/j.neuron.2009.08.018
16. Lei K, Zhang X, Ding X, Guo X, Chen M, Zhu B, Xu T, Zhuang Y, Xu R, Han M. SUN1 and SUN2 play critical but partially redundant roles in anchoring nuclei in skeletal muscle cells in mice. Proc Natl Acad Sci U S A 2009; 106:10207-12; PMID:19509342; http://dx.doi.org/10.1073/pnas.0812037106
17. Stuurman N, Heins S, Aebi U. Nuclear lamins: their structure, assembly, and interactions. J Struct Biol 1998; 122:42-66; PMID:9724605; http://dx.doi.org/10.1006/jsbi.1998.3987
18. Hutchison CJ. Lamins: building blocks or regulators of gene expression? Nat Rev Mol Cell Biol 2002; 3:848-58; PMID:12415302; http://dx.doi.org/10.1038/nrm950
19. Burke B, Roux KJ. Nuclei take a position: managing nuclear location. Dev Cell 2009; 17:587-97; PMID:19922864; http://dx.doi.org/10.1016/j.devcel.2009.10.018
20. Starr DA, Fridolfsson HN. Interactions between nuclei and the cytoskeleton are mediated by SUN-KASH nuclear-envelope bridges. Annu Rev Cell Dev Biol 2010; 26:421-44; PMID:20507227; http://dx.doi.org/10.1146/annurev-cellbio-100109-104037
21. Razafsky D, Hodzic D. Bringing KASH under the SUN: the many faces of nucleo-cytoskeletal connections. J Cell Biol 2009; 186:461-72; PMID:19687252; http://dx.doi.org/10.1083/jcb.200906068
22. Hodzic DM, Yeater DB, Bengtsson L, Otto H, Stahl PD. Sun2 is a novel mammalian inner nuclear membrane protein. J Biol Chem 2004; 279:25805-12; PMID:15082709; http://dx.doi.org/10.1074/jbc.M313157200
23. Haque F, Lloyd DJ, Smallwood DT, Dent CL, Shanahan CM, Fry AM, Trembath RC, Shackleton S. SUN1 interacts with nuclear lamin A and cytoplasmic nesprins to provide a physical connection between the nuclear lamina and the cytoskeleton. Mol Cell Biol 2006; 26:3738-51; PMID:16648470; http://dx.doi.org/10.1128/MCB.26.10.3738-3751.2006
24. Crisp M, Liu Q, Roux K, Rattner JB, Shanahan C, Burke B, Stahl PD, Hodzic D. Coupling of the nucleus and cytoplasm: role of the LINC complex. J Cell Biol 2006; 172:41-53; PMID:16380439; http://dx.doi.org/10.1083/jcb.200509124
25. Wilhelmsen K, Litjens SH, Kuikman I, Tshimbalanga N, Janssen H, van den Bout I, Raymond K, Sonnenberg A. Nesprin-3, a novel outer nuclear membrane protein, associates with the cytoskeletal linker protein plectin. J Cell Biol 2005; 171:799-810; PMID:16330710; http://dx.doi.org/10.1083/jcb.200506083
26. Roux KJ, Crisp ML, Liu Q, Kim D, Kozlov S, Stewart CL, Burke B. Nesprin 4 is an outer nuclear membrane protein that can induce kinesin-mediated cell polarization. Proc Natl Acad Sci U S A 2009; 106:2194-9; PMID:19164528; http://dx.doi.org/10.1073/pnas.0808602106
27. Padmakumar VC, Abraham S, Braune S, Noegel AA, Tunggal B, Karakesisoglou I, Korenbaum E. Enaptin, a giant actin-binding protein, is an element of the nuclear membrane and the actin cytoskeleton. Exp Cell Res 2004; 295:330-9; PMID:15093733; http://dx.doi.org/10.1016/j.yexcr.2004.01.014
28. Meyerzon M, Fridolfsson HN, Ly N, McNally FJ, Starr DA. UNC-83 is a nuclear-specific cargo adaptor for kinesin-1-mediated nuclear migration. Development 2009; 136:2725-33; PMID:19605495; http://dx.doi.org/10.1242/dev.038596
29. Fridolfsson HN, Starr DA. Kinesin-1 and dynein at the nuclear envelope mediate the bidirectional migrations of nuclei. J Cell Biol 2010; 191:115-28; PMID:20921138; http://dx.doi.org/10.1083/jcb.201004118
30. Patterson K, Molofsky AB, Robinson C, Acosta S, Cater C, Fischer JA. The functions of Klarsicht and nuclear lamin in developmentally regulated nuclear migrations of photoreceptor cells in the Drosophila eye. Mol Biol Cell 2004; 15:600-10; PMID:14617811; http://dx.doi.org/10.1091/mbc.E03-06-0374
31. Mosley-Bishop KL, Li Q, Patterson L, Fischer JA. Molecular analysis of the klarsicht gene and its role in nuclear migration within differentiating cells of the Drosophila eye. Curr Biol 1999; 9:1211-20; PMID:10556085; http://dx.doi.org/10.1016/S0960-9822(99)80501-6
32. Kracklauer MP, Banks SM, Xie X, Wu Y, Fischer JA. Drosophila klaroid encodes a SUN domain protein required for Klarsicht localization to the nuclear envelope and nuclear migration in the eye. Fly (Austin) 2007; 1:75-85; PMID:18820457
33. Fan SS, Ready DF. Glued participates in distinct microtubule-based activities in Drosophila eye development. Development 1997; 124:1497-507; PMID:9108366
34. Tsujikawa M, Omori Y, Biyanwila J, Malicki J. Mechanism of positioning the cell nucleus in vertebrate photoreceptors. Proc Natl Acad Sci U S A 2007; 104:14819-24; PMID:17785424; http://dx.doi.org/10.1073/pnas.0700178104
35. Sullivan T, Escalante-Alcalde D, Bhatt H, Anver M, Bhat N, Nagashima K, Stewart CL, Burke B. Loss of A-type lamin expression compromises nuclear envelope integrity leading to muscular dystrophy. J Cell Biol 1999; 147:913-20; PMID:10579712; http://dx.doi.org/10.1083/jcb.147.5.913
36. Jahn D, Schramm S, Schnölzer M, Heilmann CJ, de Koster CG, Schütz W, Benavente R, Alsheimer M. A truncated lamin A in the Lmna -/- mouse line: implications for the understanding of laminopathies. Nucleus 2012; 3:463-74; PMID:22895093; http://dx.doi.org/10.4161/nucl.21676
37. Röber RA, Weber K, Osborn M. Differential timing of nuclear lamin A/C expression in the various organs of the mouse embryo and the young animal: a developmental study. Development 1989; 105:365-78; PMID:2680424
38. Young SG, Jung HJ, Coffinier C, Fong LG. Understanding the roles of nuclear A- and B-type lamins in brain development. J Biol Chem 2012; 287:16103-10; PMID:22416132; http://dx.doi.org/10.1074/jbc.R112.354407
39. Göb E, Meyer-Natus E, Benavente R, Alsheimer M. Expression of individual mammalian Sun1 isoforms depends on the cell type. Commun Integr Biol 2011; 4:440-2; PMID:21966565
40. Zhang J, Felder A, Liu Y, Guo LT, Lange S, Dalton ND, Gu Y, Peterson KL, Mizisin AP, Shelton GD, et al. Nesprin 1 is critical for nuclear positioning and anchorage. Hum Mol Genet 2010; 19:329-41; PMID:19864491; http://dx.doi.org/10.1093/hmg/ddp499
41. Zhang Q, Skepper JN, Yang F, Davies JD, Hegyi L, Roberts RG, Weissberg PL, Ellis JA, Shanahan CM. Nesprins: a novel family of spectrin-repeat-containing proteins that localize to the nuclear membrane in multiple tissues. J Cell Sci 2001; 114:4485-98; PMID:11792814
42. Rajgor D, Mellad JA, Autore F, Zhang Q, Shanahan CM. Multiple novel nesprin-1 and nesprin-2 variants act as versatile tissue-specific intracellular scaffolds. PLoS One 2012; 7:e40098; PMID:22768332; http://dx.doi.org/10.1371/journal.pone.0040098
43. Young SG, Jung HJ, Coffinier C, Fong LG. Understanding the roles of nuclear A- and B-type lamins in brain development. J Biol Chem 2012; 287:16103-10; PMID:22416132; http://dx.doi.org/10.1074/jbc.R112.354407
44. Broers JL, Ramaekers FC, Bonne G, Yaou RB, Hutchison CJ. Nuclear lamins: laminopathies and their role in premature ageing. Physiol Rev 2006; 86:967-1008; PMID:16816143; http://dx.doi.org/10.1152/physrev.00047.2005
45. Wakabayashi T, Mori T, Hirahara Y, Koike T, Kubota Y, Takamori Y, Yamada H. Nuclear lamins are differentially expressed in retinal neurons of the adult rat retina. Histochem Cell Biol 2011; 136:427-36; PMID:21842415; http://dx.doi.org/10.1007/s00418-011-0853-8
46. Solovei I, Wang AS, Thanisch K, Schmidt CS, Krebs S, Zwerger M, Cohen TV, Devys D, Foisner R, Peichl L, et al. LBR and lamin A/C sequentially tether peripheral heterochromatin and inversely regulate differentiation. Cell 2013; 152:584-98; PMID:23374351; http://dx.doi.org/10.1016/j.cell.2013.01.009
47. Yoon BC, Jung H, Dwivedy A, O'Hare CM, Zivraj KH, Holt CE. Local translation of extranuclear lamin B promotes axon maintenance. Cell 2012; 148:752-64; PMID:22341447; http://dx.doi.org/10.1016/j.cell.2011.11.064
48. Göb E, Schmitt J, Benavente R, Alsheimer M. Mammalian sperm head formation involves different polarization of two novel LINC complexes. PLoS One 2010; 5:e12072; PMID:20711465; http://dx.doi.org/10.1371/journal.pone.0012072
49. Randles KN, Lam T, Sewry CA, Puckelwartz M, Furling D, Wehnert M, McNally EM, Morris GE. Nesprins, but not sun proteins, switch isoforms at the nuclear envelope during muscle development. Dev Dyn 2010; 239:998-1009; PMID:20108321; http://dx.doi.org/10.1002/dvdy.22229
50. Zhang J, Felder A, Liu Y, Guo LT, Lange S, Dalton ND, Gu Y, Peterson KL, Mizisin AP, Shelton GD, et al. Nesprin 1 is critical for nuclear positioning and anchorage. Hum Mol Genet 2010; 19:329-41; PMID:19864491; http://dx.doi.org/10.1093/hmg/ddp499
51. Guo Y, Jangi S, Welte MA. Organelle-specific control of intracellular transport: distinctly targeted isoforms of the regulator Klar. Mol Biol Cell 2005; 16:1406-16; PMID:15647372; http://dx.doi.org/10.1091/mbc.E04-10-0920
52. Yu YV, Li Z, Rizzo NP, Einstein J, Welte MA. Targeting the motor regulator Klar to lipid droplets. BMC Cell Biol 2011; 12:9; PMID:21349165; http://dx.doi.org/10.1186/1471-2121-12-9
53. Gros-Louis F, Dupré N, Dion P, Fox MA, Laurent S, Verreault S, Sanes JR, Bouchard JP, Rouleau GA. Mutations in SYNE1 lead to a newly discovered form of autosomal recessive cerebellar ataxia. Nat Genet 2007; 39:80-5; PMID:17159980; http://dx.doi.org/10.1038/ng1927
54. Ding X, Xu R, Yu J, Xu T, Zhuang Y, Han M. SUN1 is required for telomere attachment to nuclear envelope and gametogenesis in mice. Dev Cell 2007; 12:863-72; PMID:17543860; http://dx.doi.org/10.1016/j.devcel.2007.03.018
55. Kolb T, Maass K, Hergt M, Aebi U, Herrmann H. Lamin A and lamin C form homodimers and coexist in higher complex forms both in the nucleoplasmic fraction and in the lamina of cultured human cells. Nucleus 2011; 2:425-33; PMID:22033280; http://dx.doi.org/10.4161/nucl.2.5.17765
56. Khatau SB, Bloom RJ, Bajpai S, Razafsky D, Zang S, Giri A, Wu PH, Marchand J, Celedon A, Hale CM, et al. The distinct roles of the nucleus and nucleus-cytoskeleton connections in three-dimensional cell migration. Sci Rep 2012; 2:488; PMID:22761994; http://dx.doi.org/10.1038/srep00488
57. Zhang X, Xu R, Zhu B, Yang X, Ding X, Duan S, Xu T, Zhuang Y, Han M. Syne-1 and Syne-2 play crucial roles in myonuclear anchorage and motor neuron innervation. Development 2007; 134:901-8; PMID:17267447; http://dx.doi.org/10.1242/dev.02783